Title: Ten-year projection of white-nose syndrome disease dynamics at the southern leading-edge of infection in North America

Article impact statement: A projected decline in bat abundance in southern North America

Running head: WNS disease dynamics

Keywords: Chiroptera, dispersal, landscape structure, Texas, WNS, source-sink dynamics, disease management

Word count: 5,015

Author details: Melissa B. Meierhofer[1,2], Thomas M. Lilley[2*], Lasse Ruokolainen[3], Joseph S. Johnson[4], Steven Parratt[5], Michael L. Morrison[1], Brian L. Pierce[6], Jonah W. Evans[7], Jani Anttila[3]

[1]Department of Rangeland, Wildlife and Fisheries Management, Texas A&M University, 534 John Kimbrough Blvd., College Station, Texas 77843, United States; [2]Finnish Museum of Natural History, University of Helsinki, Pohjoinen Rautatiekatu 13, 00100 Helsinki, Finland; [3]Department of Biosciences, University of Helsinki, Yliopistonkatu 4, 00100 Helsinki, Finland; [4]Department of Biological Sciences, Ohio University, Athens, Ohio 45701, United States; [5]Department of Ecology and Evolution, University of Liverpool, Liverpool L69 7BE, United Kingdom; [6]Natural Resources Institute, Texas A&M University, 578 John Kimbrough Blvd. College Station, Texas 77843, United States; [7]Wildlife Diversity Program, Texas Parks and Wildlife, 4200 Smith School Road, Austin, Texas 78744, United States

Corresponding author: Thomas M. Lilley, Finnish Museum of Natural History, University of Helsinki, Pohjoinen Rautatiekatu 13, 00100 Helsinki, Finland; Thomas.lilley@helsinki.fi

Acknowledgements

D. Wright, Dr. Comer, Dr. Godwin are thanked for site access; J. Kennedy is thanked for site access and data collection; K. Demere, B. Stamps, L. Wolf, S. Goree, J. Carey are thanked for field assistance in data collection. Funding for this project was provided through the U.S. Fish and Wildlife Service's State Wildlife Grant Program (CFDA# 15.611) as administered by Texas Parks and Wildlife Department and the U.S. Fish and Wildlife Service's (Service) CFDA Program (15.657). Additional funding was provided by the fightWNS 'Micro Grants for Microbats' and the NSS WNS Rapid Response Fund. This work was supported by the Fulbright Finland Foundation and Finnish National Agency for Education EDUFI (MBM) and the Academy of Finland (TML, grant# 331515).

Abstract

Predicting the emergence and spread of infectious diseases is critical for effective conservation of biodiversity. White-nose syndrome (WNS), an emerging infectious disease of bats, has resulted in high mortality in eastern North America. Because the fungal causative agent *Pseudogymnoascus destructans* is constrained by temperature and humidity, spread dynamics may vary greatly by geography. Environmental conditions in the southern part of the continent, where disease dynamics are typically studied, making it difficult to predict how the disease will manifest. Herein, we modeled the spread of WNS in Texas based on available cave densities and average dispersal distances of species occupying these sites, and projected these results out to 10 years. We parameterized a predictive model of WNS epidemiology and its effects on hibernatory bat populations with observed environmental data from bat hibernation sites in Texas. Our model suggests that bat populations in northern Texas will be more affected by WNS mortality than

47 southern Texas. As such, we recommend prioritizing the preservation of large overwintering
48 colonies of bats in north Texas through management actions. Our model further illustrates that
49 infectious disease spread and infectious disease severity can become uncoupled over a gradient
50 of environmental variation. Finally, our results highlight the importance of understanding host,
51 pathogen and environmental conditions in various settings to elucidate what may happen across a
52 breadth of environments.
53
54
55 **Introduction**
56 Emerging infectious diseases (EID) of wildlife are increasing in number and threatening
57 several species with extinction (Hayman et al. 2013; Hoberg & Brooks 2015; Tompkins et al.
58 2015). Emerging infectious diseases are those newly appearing or rapidly increasing in a
59 population (Morse 2004). EIDs occur when pathogenic or putatively pathogenic organisms in the
60 environment have the opportunity to infect new hosts species or populations. Changing
61 environmental conditions can accelerate this process of host-switching by driving changes in
62 host-species' distributions and by creating new habitable environmental reservoir pathogens
63 (Morse 1991; 1993). Emergence of infectious diseases are therefore associated with a range of
64 causal factors, including ecosystem alterations and movements of pathogens or vectors (Morse
65 1995). The spread of EIDs is mediated by differences in host ecology, resulting in various
66 patterns of spatial spread (Smith et al. 2002; LaDeau et al. 2008; Meentemeyer et al. 2011).
67 Therefore, understanding and predicting the spatial structure of future EID epidemics requires
68 integration of both the environmental factors and species-specific ecology that can underpin
69 pathogen contact networks (Parratt et al. 2016).

Modeling the spread of EIDs can guide and improve upon effective, science-based management and conservation practices and efforts by identifying key factors driving pathogen persistence and disease dynamics (Keeling & Rohani 2007; Perez & Dragicevic 2009). Although predictive power depends on the accuracy of the data used, models can provide predictive information to target conservation and control measures where the pathogen exists and plan adaptive management strategies where the pathogen may spread (Keeling & Rohani 2007; Cunniffe et al. 2016). These targeted measures can be used to improve the efficacy of conservation measures and help to eradicate infections from the population, protecting host biodiversity (Keeling & Rohani 2007).

An EID of bats known as white-nose syndrome (WNS) threatens the survival of populations of several cave-hibernating species in North America (Gargas et al. 2009; Lorch et al. 2011; Warnecke et al. 2012). Since the first documentation in North America in winter 2006–2007, the fungal causative agent *Pseudogymnoascus destructans* has spread at a rate of 200 to 900 km per year, and is associated with mortality in excess of 90% (Gargas et al. 2009; Foley et al. 2011; Ingersoll et al. 2013). The first documentation of the disease occurred in Howes Cave near Albany, New York in February 2006, and it has since been documented across a substantial portion of North America (Blehert et al. 2009; Turner & Reeder 2009; Lorch et al. 2016). Although, bat-to-bat transmission is the primary mode of disease dispersal (Raudabaugh & Miller 2013), *P. destructans* can persist in an environment devoid of bats (Minnis & Linder 2013; Hoyt et al. 2015; Leopardi et al. 2015). The disease disrupts hibernation behavior through multiple pathways (Verant et al. 2014; Field et al. 2015; Lilley et al. 2017) leading to an increased arousal frequency and ultimately, the depletion of fat reserves (Reeder 2012). This has generated predictions of local extirpations and extinctions of once common bat species (Ingersoll

et al. 2016; Pettit & O'Keefe 2017; Frank et al. 2019). There is therefore a need to understand future spread so that conservation efforts can be best prioritized. Moving towards this understanding will require study of how factors associated with WNS transmission work together to influence spread.

The vegetative growth of *P. destructans* is constrained by temperature and humidity (Verant et al. 2012; Marroquin et al. 2017), hence certain environments may not be optimal for growth and thus impede spread. Factors known to be associated with the transmission of the fungus include bat species composition and abundance, population composition (Lilley et al. 2020), geography (e.g., connectivity of hibernacula), and climate (Wilder et al. 2011; Langwig et al. 2012; Maher et al. 2012; Lilley et al. 2018). As a result, the dynamics of WNS disease spread may vary greatly by geography and demography. Predictive modelling of WNS has focused on northeastern United States (e.g., Flory et al. 2012), or used data from that region to parameterize their disease-spread models in other regions (e.g., Maher et al. 2012). Consequently, findings from these studies may not reflect regional differences among bat hibernacula (McNab 1974; Humphries et al. 2002; Brack 2007). It is therefore important to understand and analyze the incidence—and prevalence of—WNS over different spatial and temporal scales to more accurately determine the potential impacts of disease in those regions (Perez & Dragicevic 2009).

Texas provides a unique situation for studying disease spread in that it has the greatest number of bat species of any state in the United States and many of these species were naïve to *P. destructans* until spring 2017, with *P. destructans* documented in the farthest southern locality at 30 parallel north in Texas (Schmidly & Bradley 2016; TPWD 2017, 2019). WNS invasion of Texas is ongoing, with infection first documented during spring 2020 (TPWD 2020). Despite

116 this, minimal information currently exists on whether the environmental conditions in potential
117 bat hibernacula (i.e., caves) (Meierhofer et al. 2019), the spatial layout of caves, and the
118 frequency of suitable caves in the landscape for the persistence of *P. destructans* in the
119 environment in Texas are conducive to the persistence of WNS. It is important to acknowledge
120 that *P. destructans* can exist in the environment without infecting the bat host or causing
121 mortality due to WNS (Lorch et al. 2013b; Hoyt et al. 2015). Unlike the northeast, there has not
122 yet been substantial mortality documented or reported resulting from WNS in Texas. Due to a
123 sense of urgency resulting from the mass declines documented in other regions of North
124 America, researchers are currently deploying treatments in Texas hibernacula as a management
125 strategy to prevent pathogen exposure and to reduce disease severity. Several of these treatments
126 are being deployed in culverts, which are inherently easier to treat in comparison to caves due to
127 their simple design and ease of access. Thus, understanding whether WNS can develop in certain
128 regions in Texas and how the disease will move throughout the southern region is integral in
129 implementing proper conservation and management strategies for caves.
130 Here, we used demographic and environmental data collected from caves at the leading
131 edge of WNS spread in Texas to parametrize a novel predictive model of fungal epidemiology.
132 To simplify the model and provide robust predictions, our modeling approach does not
133 investigate specific bat species, but combines all species. As such, we refer to a population as all
134 cave-hibernating species combined. Furthermore, using environmental data from caves and
135 PRISM climate data we model the probability of *P. destructans* being able to infect their hosts,
136 leading to symptoms of WNS, and furthermore, the death of the host. Herein, we hypothesized
137 that (1) spread is accelerated by high cave concentrations and bat abundance and (2) disease
138 development is hindered by internal and external environmental conditions affecting both bat

ecology and fungal growth. We projected our results 10 years ahead to provide stakeholders information on how the disease will most likely behave to better implement conservation measures.

Materials and Methods

In Texas where greater than 95% of land is privately owned, caves, as opposed to other hibernacula (e.g., culverts, buildings), are challenging to monitor and manage for WNS because of access restrictions. As such, we focused solely on caves for model development as opposed to other potential hibernacula because of the lack of available data on environmental characteristics of alternative hibernacula across a broad geographic range in Texas and to retain the simplicity of the model.

Model Development

Our mathematical model is a modification of the model published by Lilley et al. (2018). In comparison with the previously published model, we have simplified the hibernation and transmission dynamics to achieve easier parameterization, and do not consider environmental stochasticity (Supporting Information). The model consists of differential equations, with a periodic temperature forcing, describing the dynamics of the bat hosts and the free pathogenic fungus. We divided the hosts into susceptible, exposed, and infectious, all of which can be either active or hibernating, leading to seven compartments in total. The dynamic state is tracked in a network of patches representing caves within the counties of Texas. We implemented in C++ and full program codes are available at https://github.com/janivaltteri/wnstexas. The full model description is provided in Supporting Information.

161 To utilize the model on Texas topography, we initially assumed all documented caves
162 could be hibernation sites, and assigned the estimated 4251 hibernation sites obtained from the
163 Texas Speleological Survey database to 94 counties from which we had environmental data.
164 Inside each county (a geographical region used for administrative purposes), we grouped
165 hibernation sites according to cave mean temperatures into bins of 2 °C, following a gaussian
166 distribution with county-specific mean and variance of 3.75 °C. We estimated the mean cave
167 temperature based on a linear model of mean ambient temperature and cave coordinates
168 (Supporting Information). We then used this model to predict mean cave temperatures for the
169 geographic centers of each county. We used the variance of the model residuals to estimate the
170 3.75 °C variance.
171 We considered each 2 °C bin of caves as a patch *i* in county *j* with carrying capacity $K_{i,j}$
172 given by the number of hibernation sites in that bin (Fig. 1). We did not assume that all caves
173 were occupied by bats, but rather approximated that 40% of caves were occupied based on our
174 survey data. In total, there were 303 patches. Hibernaculum temperature inside each patch varied
175 sinusoidally with an amplitude estimated for each county (Supporting Information), affecting
176 fungal growth rates inside the hibernaculum. In addition, we assigned each county a mean
177 ambient temperature and annual sinusoidal variation, according to a linear fit (of Fourier
178 coefficients) on the PRISM data.
179 We implemented patch-to-patch migration (dispersal) as follows: each patch had a fixed
180 proportion of susceptible and exposed bats emigrating per day. To retain simplicity of the model,
181 we do not directly account for species structure variation nor movement among sites during
182 winter. We divided the emigrating bats into recipient patches depending on distance. We
183 assigned a weight $w_{i\to k,j\to l} = K_{k,l}e^{-\gamma d_{i\to k,j\to l}}$, where $d_{i\to k,j\to l}$ is the distance from patch *i* in

184 county j to patch k in county l for each connection under a cutoff distance of 100 km, and we
185 calculated the proportion going to a target patch as $\pi_{i\to k,j\to l} = w_{i\to k,j\to l} / \left(\left(K_{i,j} - 1\right) e^{-\gamma d_{j\to j}} + \right.$
186 $\left. \sum_{n,m} w_{i\to n,j\to m} \right)$. We calculated patch to patch distances $d_{j\to j}$ within a county as mean distances
187 of two randomly placed points inside the county. Distances between counties were simply the
188 distances between the two county midpoints. The parameter γ scales the recipient patch
189 distribution with respect to distance from the focal patch. Under our validated parameter set we
190 used a γ value of 0.00868 km^{-1}.

191 Hibernation strongly affects disease dynamics because *P. destructans* has different
192 effects on active and hibernating bats (Hayman et al. 2016). We determined the duration of
193 hibernation in a patch by ambient and hibernaculum temperatures, T_{amb} and T_{hib}, together with
194 three threshold values α. A patch is in hibernation when either $T_{amb}(t) < \alpha_{amb,0}$ or $T_{amb}(t) <$
195 $\alpha_{amb,1}$; $T_{hib}(t) < \alpha_{hib}$. Our parameter set used threshold values $\alpha_{amb,0}$, α_{hib} = 11.5 °C and $\alpha_{amb,1}$
196 = 12.5 °C (Perry 2013; Meierhofer et al. 2019).

197 We used a simple linear force of infection in response to environmental fungal density
198 instead of the more sophisticated sigmoidal response used in the model of Lilley et al. (2018).
199 Additionally, we have resorted to simple threshold functions for bat population growth rate and
200 the transfer rates between active and hibernation states. While the original formulation in Lilley
201 et al. (2018) is theoretically sound and results in smoother dynamics, our current formation is
202 analytically more tractable/computationally better suited to integrating real-world variation in
203 parameters. The sigmoidal infectivity response has, however, notable effects on disease
204 dynamics. Therefore, we have replicated all simulation experiments using different sigmoidal
205 parameterizations, and show the resulting effects in Supporting Information.

We visualized model predictions in R with interpolated heat maps generated by the linear bivariate method in the package `akima::interp()` on an 80x80 grid under default settings. Interpolation predicts values within a convex hull bounding the data points. Therefore, we did not predict beyond the spatial extremes of the data produced by the predictive model described above. We plotted infection as the carrying-capacity scaled predictions from the infection model at 5 and 10 years of simulation, and calculated the loss of bat abundance as the proportional reduction in bats predicted by the infection model relative to a no-infection scenario, obtained by running the model without the fungus and initial infections. We used functions in the `Raster` and `ggplot2` packages to create the figures.

Model Parameters and Parametrization

We obtained information on number of caves per county within Texas from the Texas Speleological Survey (TSS, https://www.texasspeleologicalsurvey.org/). The TSS, Texas Cave Management Association, local Grottos, biologists, and private landowners provided access to specific cave sites for data collection.

We gathered daily mean ambient temperature data for each county from 1 January 2017 to 31 December 2018 from PRISM (PRISM Climate Group 2018). We used EL-USB-2 Data loggers (Lascar Electronics Inc.) placed within the first third of each cave near roosting bats, when present, to record internal ambient temperature every hour for one year. We deployed loggers at each of 27 caves (13 caves occupied by hibernating bats, 14 unoccupied) distributed in 19 counties across north and central Texas where permission was obtained. We placed loggers near bats or centrally in caves where bats were not present. We obtained information on presence *of P. destructans* within a county from Texas Parks and Wildlife Department (TPWD 2019).

228 We determined bat and fungal parameter values (Table 1) roughly based on those
229 estimated by Lilley et al. (2018). For our model, we focused solely on using information on bat
230 species known to hibernate in Texas (hibernatory bat populations) as bats that hibernate are
231 affected by WNS. The average number of non-Mexican free-tailed bats (*Tadarida brasiliensis*)
232 was calculated to be 344 based on data collected on bat counts during our previous survey efforts
233 of caves in Texas. We disregarded Mexican free-tailed bat colonies as this species does not tend
234 to hibernate. With our previous survey counts, and documentation of large bat colonies by other
235 researchers (e.g., Tinkle & Milstead 1960; Ammerman et al. 2012; Caire et al. 2019), we
236 approximated that the average number of bats per cave to be 900 for the purpose of our model.
237 Direct assignment of parameter values to our model for the actual biological setting
238 would have been challenging because many of the needed values are not known or directly
239 measurable. Instead, we used literature-based values and approximated values of the authors in
240 combination with a parameter estimation step based on the known initial state of the disease in
241 2018 and survey data from 2020. With the estimation step, we ensured that our parameter set
242 would predict the 2020 observed state from the initial conditions, and thus be in line with the
243 actual known WNS disease dynamics in Texas.
244 To parameterize the model, we started by constructing a parameter set, which represented
245 our best knowledge of the model parameter values obtained by averaging approximated values of
246 the co-authors (Table 1). We then refined our estimates with an approximate Bayesian
247 computation procedure (Sunnåker et al. 2013). First, we constructed a prior distribution by
248 assigning to each of the parameter values a log-Gaussian distribution with our estimate as the
249 median value and a log-unitary standard deviation, following the reasoning that the true
250 parameter values fall within one order of magnitude from our initial estimate. We then ran 500

simulations with parameters randomly drawn from our prior distributions (Supporting Information) and performed rejection sampling to select appropriate posterior combinations based on WNS 2020 survey data (Fig. 2). With no easy way of assigning likelihood values to our simulations, we used simple rejection thresholds. We used <0.1% disease prevalence in counties where WNS in bats was detected as the rejection criteria, following the reasoning that a small prevalence in bats could already be detected through surveys. We further used <20% free-living fungus prevalence in counties where *P. destructans* was detected as the rejection criteria, because finding fungal growth outside of the bat hosts requires active search of hibernation sites after 2 years of simulation time. Our threshold values were admittedly arbitrary because we had no information on the actual detection effort or efficiency, but these values can easily be improved in future work. Additionally, there were two counties surveyed with neither WNS or *P. destructans* were detected, and we rejected >0.1% disease prevalence and >20% free-living fungus prevalence in these. We then used parameter median values from the accepted combinations (with 5% acceptance rate) as our validated parameter set. We fixed hibernation rate and threshold parameters to our literature-based estimates and were not found by this validation step. We studied the robustness of our results separately in a sensitivity analysis (Supporting Information), where we investigated how varying each parameter by a small increment or decrement changes the simulation outcome in terms of the number of affected patches and reduction in bat numbers.

Results

Under our parameter set validated against 2020 WNS survey data, the hibernatory bat population declined 35.6% across 84 counties in 10 years (Fig. 3). After five years, the bat

274 population would be reduced by 19.3% in 70 counties. The simulations did not show local
275 extinctions in any county, but the bat population reduced by 86% (85% after five years) in the
276 most affected site. The most affected counties were in north Texas, with *P. destructans* present at
277 the start of the simulation. The bat population rich mid-Texas are projected to lose between one
278 quarter to half of the bat population (Figs. 3cd, 4a). Density of the free-living fungus and its
279 spores reached high levels in the bat population rich counties (Fig. 4b).
280 *Pseudogymnoascus destructans* caused low mortality in the southernmost counties under
281 our parameter set. This is because high ambient temperatures did not support long enough
282 hibernation periods for significant disease progression to the infectious state (Fig. 4a). The warm
283 temperatures and resulting short hibernation period also reduced the impact of the epidemic in
284 the central-Texas counties. While cold patches may have periods of hibernation even in warm
285 counties, the cave temperature was then below optimal (13.0 °C, Verant et al. 2012) for fungal
286 growth. Exposed bats carrying the fungus will be present, however, because of dispersal from
287 affected sites.
288 While both transmission modes—environmental and direct—are significant components
289 of epidemic spread, under our parameterization transmission via the environment had a larger
290 impact, causing approximately 90% of the force of infection along the simulation time
291 (Supplementary Material). However, sensitivity analysis on the infectivity parameters shows that
292 similar results can be obtained by decreasing one parameter and increasing the other parameter
293 (i.e., adjusting rate parameters associated with the two transmission modes; Supplementary
294 Material). Removing environmental transmission from the model resulted in 99% less bat
295 population reduction after 10 years. This occurs because most of the exposed and infected bats
296 shed the fungus and revert back to the susceptible state during the summer, and transmissions

297 from the environment is required to re-infect the bat population at the start of hibernation period.
298 However, direct transmission still impacted the bat population; removing direct transmission
299 resulted in 90% less bat population reduction. Direct transmission is the most probable cause of
300 the disease spread into new counties. When exposed bats disperse into new sites, they shed
301 fungus into the environment, but also transmit directly to susceptible hosts when entering
302 hibernation. Because fungal densities remain low in the environment at new sites initially, the
303 direct transmission route may be more prevalent.

304 The sensitivity analysis shows that the spread of WNS changes under variation of the
305 parameters. Specifically, our results are most susceptible to changes in direct transmission rate,
306 infection rate, and hibernation temperature thresholds, which increase the disease mortality and
307 spread when the parameter value increases, and bat growth rate, which decreases mortality and
308 spread when the parameter value increases. Increasing the mean dispersal distance (decreasing γ)
309 significantly increases the number of affected patches, but does not significantly affect mortality.
310

311 **Discussion**

312 Our predictive models found that mortality due to WNS will vary across Texas cave
313 hibernacula, with northern sites more affected than southern sites. Results from our model
314 suggest that in 5 to 10 years, we can expect to see a substantial (>75%) reduction in the number
315 and size of bat populations in the northern sites because of an increase in mortality due to this
316 fungal disease. Central sites are affected to a lesser degree, with a model projected 30–50%
317 reduction in population densities, whereas southern sites are mostly unaffected. Interestingly, the
318 free-living fungus reaches very high densities in central Texas where hibernation sites are most
319 numerous, but due to warm temperatures, the bat populations in these sites are less severely

affected likely due to shorter periods of torpor. The high fungal densities are in part explained by the reduced mortality, resulting in a long duration during which bats shed fungal spores.

The first documentation of WNS was anticipated to be in north Texas based on environmental characteristics (Meierhofer et al. 2019) and proximity to nearest WNS-infected sites. However, WNS was first documented on cave myotis (*Myotis velifer*) in 18 counties in central Texas in spring 2020 (TPWD 2020; Fig. 2). This is the first documentation of WNS in central and southern regions, resulting after four years of *P. destructans* being present in Texas. The finding of WNS in central Texas does support our model in that some regions in central Texas will have hibernacula conducive to WNS development. Our model shows that both the fungus and WNS are prevalent in central Texas, but that the proportional disease mortality is smaller in central Texas than in northern Texas. Despite the low mortality in comparison to north Texas, our model suggests that *P. destructans* reaches higher densities in central Texas than in northern Texas because fewer exposed bats succumb to the disease, increasing the continued spread of the fungus. Central Texas has the greatest abundance of known hibernacula in Texas, as well as the greatest diversity of bats in the state (Ammerman et al. 2012), increasing the potential for infection susceptibility to the disease for some bat species. Unfortunately, the origin (hibernacula) for most of the WNS positive bats is unknown, with some found—for example—outside of a house (6%), at a bridge (9%), submitted for rabies testing (31%), and on a path (3%) (J. Evans pers. com.). These WNS positive bats were found in February, suggesting these bats were recently in hibernation. However, it is still difficult to determine whether the first hibernacula with WNS are located within central Texas or elsewhere.

Our model suggests that the WNS epidemic is dependent on exposure to the spores in the environment. Indeed, contact of bats with the contaminated environment (Linder et al. 2011;

343 Lorch et al. 2013a, 2013b) in autumn has been shown to initiate the infection (Langwig et al.
344 2015). Our findings further complement recent findings suggesting that persistence of high levels
345 *P. destructans* in the environment result in widespread infections (Hoyt et al. 2020). Although
346 the primary method of spread of *P. destructans* and WNS is bat-to-bat (Raudabaugh & Miller
347 2013), under our parameter set only 1 in 10 is due to direct contact to an infectious individual
348 during hibernation. The overall pattern is not very sensitive to the relative strengths of these two
349 components (modes of pathogen spread: environmental, direct) and temporally detailed data
350 would be required to estimate these parameters independently. This is important to note,
351 however, as indirect and infrequent transmission (cryptic connections) play a key role in the
352 transmission and community-wide spread of *P. destructans* (Hoyt et al. 2018). One factor that
353 may have resulted in the reduction in bat-to-bat transmission in our model is our choice to not
354 include information about the Mexican free-tailed bat. Mexican free-tailed bats could greatly
355 hasten the spread of WNS in Texas due to the proclivity to roost in large numbers, state-wide
356 distribution, and the overlap of this species with other known WNS-affected species in cave sites
357 (Ammerman et al. 2012). Although this species is not known to be impacted by WNS, it is a
358 known carrier (TPWD 2018; 2019).

359 *Pseudogymnoascus destructans* can persist in environments in the absence of a bat host
360 (Hoyt et al. 2015) with growth of *P. destructans* in colonies with long hibernation periods and in
361 sites with high levels of organic detritus (Reynolds et al. 2015). Our results suggest that reducing
362 fungal spore loads in hibernation sites may work as an effective way to slow down the epidemic
363 spread. In north Texas where temperatures are lower than in more southern regions, bats may be
364 experiencing longer hibernation periods than bats in southern regions. Susceptibility to the
365 disease requires bats to stay in torpor for prolonged periods, suggesting that pathological

366 infection occurs in regions with long periods of low ambient temperature (Ehlman et al. 2013).
367 Indeed, knowledge of hibernation temperatures of several species in Texas (Meierhofer et al.
368 2019) supports the notion of extended periods of torpor of bats in north Texas than in central and
369 southern regions of Texas. Further, the known largest bat colonies in the world exist in Texas
370 (Ammerman et al. 2012; Schmidly & Bradley 2016), with some colonies of hibernating bat
371 species occurring statewide in the thousands (e.g., tri-colored bat (*Perimyotis subflavus*), Sandel
372 et al. 2001) to tens of thousands (e.g., cave myotis (*M.* velifer), Caire et al. 2019). These large
373 colonies can provide environments conducive to the persistence of organic detritus, supporting
374 vegetative growth of *P. destructans* and creating sources of increased potential environmental
375 transmission (Reynolds et al. 2015).

376 Our model illustrates that infectious disease spread and infectious disease severity can
377 become uncoupled over a gradient of environmental variation. This is particularly a product of
378 the opportunistic nature of *P. destructans* and WNS. Whereas our model suggests some central
379 and southern counties in Texas are less affected in terms of mortality, bats still have the potential
380 to be exposed to *P. destructans* as some areas will have the fungus present. This is indicative of
381 source-sink dynamics, with infected hibernacula in the north acting as sink populations and
382 hibernacula farther south acting as source populations. The prevalence of disease as well as
383 disease invasion rate are slow in spatially clustered landscapes (Lilley et al. 2018), as reflected in
384 central Texas where densities of caves are greater than that of north Texas. However, movement
385 among sites during winter (Boyles et al 2006), as well winter emergence by bats afflicted by the
386 disease, may further the spread of WNS to uninfected areas. In southern regions of the United
387 States such as Texas where winter activity is more common than that of northern United States
388 (Bernard & McCracken 2017), these dynamics may be further exacerbated.

389 Our model-based projections are dependent on our parameterization of the dynamical
390 model. Finding the relevant parameter set for a particular case is admittedly difficult, despite that
391 for some parameters the values were readily available from previous work (Lilley et al. 2018). In
392 addition, we performed an additional validation step to refine our estimates based on
393 observations of disease spread after two years since introduction to Texas. Our initial best-
394 estimate parameter values undershot the observed pattern of disease prevalence in 2020, and the
395 refined estimates after validation led to faster spread and less lethal disease (Supporting
396 Information). The values we chose for rejection thresholds (rejection criteria) also reflect our
397 subjective views of at which level of prevalence the WNS disease and *P. destructans* would be
398 detected with the effort the surveys were performed. Similar analysis and model projections
399 could be performed with our model framework in the following years when new data become
400 available, thereby refining and improving estimates and predictions.
401 We anticipate that the spread of *P. destructans* will be slow and display source-sink
402 dynamics in Texas and at more southern regions such as northern Mexico. We further anticipate
403 that the spread of *P. destructans* in central Texas—where caves are more clustered—will be
404 similar to eastern United States, where the spread increased with proximity to nearest infected
405 site (Ingersoll et al. 2016). Indeed, results from our model suggest that conservation actions
406 should consider sites that have temperatures conducive to hibernation and suitable for fungal
407 growth, as these sites may be more susceptible to local extinctions given source-sink dynamics.
408 In light of these factors, and that large colonies of bats in temperatures suitable for *P. destructans*
409 experience the greatest impacts of WNS (Wilder et al. 2011), we recommend prioritizing the
410 preservation of large overwintering colonies of bats in north Texas through management actions.
411 We further propose that future work should focus on within-season movement movements of

412 cavernicolous bat species forming large colonies at southern latitudes to ascertain infectiousness,
413 and thus the rate of spread amongst these populations.
414
415 **Supporting Information**
416 Model description and additional analyses (Appendix S1), Hibernaculum temperature modelling
417 (Appendix S2) are available online. The authors are solely responsible for the content and
418 functionality of these materials. Queries (other than the absence of the material) should be
419 directed to the corresponding author.
420
421 **Literature Cited**
422 Akima H. 1978. A method of bivariate interpolation and smooth surface fitting for irregularly
423 distributed data points. ACM Transactions on Mathematical Software 4:148–159.
424 Ammerman LK, Hice CL, Schmidly DJ. 2012. Bats of Texas. Texas A&M University Press,
425 College Station.
426 Bernard GF, McCracken GF. 2017. Winter behavior of bats and the progression of white-nose
427 syndrome in the southeastern United States. Ecology and Evolution **7:**1487–1496.
428 Blehert DS, et al. 2009. Bat white-nose syndrome: an emerging fungal pathogen? Science
429 **323:**5911.
430 Boyles JG, Dunbar MB, Whitaker Jr JO. 2006. Activity following arousal in winter in North
431 American vespertilionid bats. Mammal Review **36:**267–280.
432 Brack V. 2007. Temperatures and locations used by hibernating bats, including *Myotis sodalis*
433 (Indiana bat), in a limestone mine: implications for conservation and management.
434 Environmental Management **40:**739–746.

435 Caire W, Loucks LS, Shaw JB, Evans JW, Gillies KE, Caywood MA. 2019. Variation in the
436 number of hibernating cave myotis (*Myotis velifer*) in western Oklahoma and
437 northwestern Texas caves prior to the arrival of white-nose syndrome. Southwestern
438 Naturalist **63:**124–132.
439 Carpenter GM, Willcox EV, Bernard RF, Stiver WH. 2016. Detection of *Pseudogymnoascus*
440 *destructans* on free-flying male bats captured during summer in the southeastern USA.
441 Journal of Wildlife Diseases **52:**922–926.
442 Cunniffe NJ, Cobb RC, Meentemeyer RK, Rizzo DM, Gilligan CA. 2016. Modeling when,
443 where, and how to manage a forest epidemic, motivated by sudden oak death in
444 California. Proceedings of the National Academy of Sciences **113:**5640–5645.
445 Ehlman SM, Cox JJ, Crowley PH. 2013. Evaporative water loss, spatial distributions, and
446 survival in white-nose-syndrome-affected little brown myotis: a model. Journal of
447 Mammalogy **94:**572–583.
448 Field KA, et al. 2015. The white-nose syndrome transcriptome: activation of antifungal host
449 responses in wing tissue of hibernating little brown myotis. PLOS Pathogens
450 **11:**e1005168.
451 Flory AR, Kumar S, Stohlgren TJ, Cryan PM. 2012. Environmental conditions associated with
452 bat white-nose syndrome mortality in the north-eastern United States. Journal of Applied
453 Ecology **49:**680–689.
454 Foley J, Clifford D, Castle K, Cryan P, Ostfeld RS. 2011. Investigating and managing the rapid
455 emergence of white-nose syndrome, a novel, fatal, infectious disease of hibernating bats.
456 Conservation Biology **25:**223–231.

457 Frick WF, et al. 2015. Disease alters macroecological patterns of North American bats. Global
458 Ecology and Biogeography **24:**741–749.
459 Fuller NW, Reichard JD, Nabhan ML, Fellows SR, Pepin LC, Kunz TH. 2012. Free-ranging
460 little brown myotis (*Myotis lucifugus*) heal from wing damage associated with white-nose
461 syndrome. EcoHealth **8:**154–162.
462 Gargas A, Trest MT, Christensen M, Volk TJ, Blehert DS. 2009. *Geomyces destructans* sp. nov.
463 associated with bat white-nose syndrome. Mycotaxon **108:**147–154.
464 Hayman DTS, Pulliam JRC, Marshall JC, Cryan PM, Webb CT. 2016. Environment, host, and
465 fungal traits predict continental-scale white-nose syndrome in bats. Science Advances
466 **2:**e1500831.
467 Hayman DTS, Bowen RA, Cryan PM, McCracken GF, O'Shea TJ, Peel AJ, Gilbert A, Webb
468 CT, Wood JLN. 2013. Ecology of zoonotic infectious diseases in bats: current knowledge
469 and future directions. Zoonoses Public Health **60:**2–21.
470 Hoberg EP, Brooks DR. 2015: Evolution in action: climate change, biodiversity dynamics and
471 emerging infectious disease. Philosophical Transactions of the Royal Society B:
472 Biological Sciences **370:**20130553.
473 Hoyt JR, Langwig KE, Okoniewski J, Frick WF, Stone WB, Kilpatrick AM. 2015. Long-term
474 persistence of *Pseudogymnoascus destructans*, the causative agent of white-nose
475 syndrome, in the absence of bats. EcoHealth **12:**330–333.
476 Hoyt JR, et al. 2020. Environmental reservoir dynamics predict global infection patterns and
477 population impacts for the fungal disease white-nose syndrome. Proceedings of the
478 National Academy of Sciences **117:**7255–7262.

479 Hoyt JR, et al. 2018. Cryptic connections illuminate pathogen transmission within community
480 networks. Nature **563:**710–713.
481 Humphries MM, Thomas DW, Speakman JR. 2002. Climate-mediated energetic constraints on
482 the distribution of hibernating mammals. Nature **418:**313–316.
483 Ingersoll TE, Sewall BJ, Amelon SK. 2013. Improved analysis of long-term monitoring data
484 demonstrates marked regional declines of bat populations in the eastern United States.
485 PLOS One **8:**e65907.
486 Ingersoll TE, Sewall BJ, Amelon SK. 2016. Effects of white-nose syndrome on regional
487 population patterns of 3 hibernating bat species. Conservation Biology **5:**1048–1059.
488 Keeling MJ, Rohani P. 2007. Modeling infectious diseases in humans and animals. Princeton
489 University Press, Princeton.
490 LaDeau SL, Marra PP, Kilpatrick AM, Calder CA. 2008. West Nile virus revisited:
491 consequences for North American ecology. BioScience **58:**937–946.
492 Langwig KE, Frick WF, Bried JT, Hicks AC, Kunz TH, Kilpatrick AM. 2012. Sociality, density-
493 dependence and microclimates determine the persistence of populations suffering from a
494 novel fungal disease, white-nose syndrome. Ecology Letters **15:**1050–1057.
495 Langwig KE, et al. 2015. Host and pathogen ecology drive the seasonal dynamics of a fungal
496 disease, white-nose syndrome. Proceedings of the Royal Society B-Biological Sciences,
497 **282:**20142335.
498 Leopardi S, Black D, Puechmaille SJ. 2015. White-nose syndrome fungus introduced from
499 Europe to North America. Current Biology **25:**R217–R219.

500 Lilley TM, Prokkola JM, Johnson JS, Rogers EJ, Gronsky S, Kurta A, Reeder DM, and Field
501 KA. 2017. Immune responses in hibernating little brown myotis (*Myotis lucifugus*) with
502 white-nose syndrome. Proceedings of the Royal Society B **284**:20162232.
503 Lilley TM, Anttila J, Ruokolainen L. 2018. Landscape structure and ecology influence the spread
504 of a bat fungal disease. Functional Ecology **32:**2483–2496.
505 Lilley TM, Sävilammi TM, Ossa G, Blomberg A, Vasemägi A, Yung V, Vendrami DLJ,
506 Johnson JS. 2020. Population connectivity predicts vulnerability to white-nose syndrome
507 in the Chilean myotis (*Myotis chiloensis*) - a genomics approach. G3-Genes Genomes
508 Genetics. **10**:2117–2126.
509 Lorch JM, et al. 2011. Experimental infection of bats with *Geomyces destructans* causes white-
510 nose syndrome. Nature **480:**376–378.
511 Lorch JM, Linder DL, Gargas A, Muller LK, Minnis AM, Blehert DS. 2013a. A culture-based
512 survey of fungi in soil from bat hibernacula in the eastern United States and its
513 implications for detection of *Geomyces destructans*, the causal agent of bat white-nose
514 syndrome. Mycologia **105:**237–252.
515 Lorch JM, Muller LK, Russell RE, O'Connor M, Linder DL, Blehert DS. 2013b. Distribution
516 and environmental persistence of the causative agent of white-nose syndrome, *Geomyces*
517 *destructans*, in bat hibernacula of the eastern United States. Applied Environmental
518 Microbiology **79:**1293–1301.
519 Lorch JM, et al. 2016. First detection of bat white-nose syndrome in western North America.
520 mSphere **1:**e00148-16.

521 Maher SP, Kramer AM, Pulliam JT, Zokan MA, Bowden SE, Barton HD, Magori K, Drake JM.
522 2012. Spread of white-nose syndrome on a network regulated by geography and climate.
523 Nature Communications **3:**1306.
524 Marroquin CM, Lavine JO, Windstam ST. 2017. Effect of humidity on development of
525 Pseudogymnoascus destructans, the causal agent of bat white-nose syndrome.
526 Northeastern Naturalist **24:**54–64.
527 McNab BK. 1974. The behavior of temperate bats in a subtropical environment. Ecology
528 **55:**943–958.
529 Meentemeyer RK, Cunniffe NJ, Cook AR, Pilipe JAN, Hunter RD, Rizzo DM, Gilligan CA.
530 2011. Epidemiological modeling of invasion in heterogeneous landscapes: spread of
531 sudden oak death in California (1990-2030). Ecosphere **2:**1–24.
532 Meierhofer MB, Johnson JS, Leivers SJ, Pierce BL, Evans JW, Morrison ML. 2019. Winter
533 habitats of bats in Texas. PLOS One **14:**e0220839.
534 Minnis AM, Linder DL. 2013. Phylogenetic evaluation of *Geomyces* allies reveals close relatives
535 of *Pseudogymnoascus destructans*, comb. nov., in bat hibernacula of eastern North
536 America. Fungal Biology **117:**638–649.
537 Morse SS. 1991. Emerging viruses: defining the rules for viral traffic. Perspectives in Biology
538 and Medicine **34:**387–409.
539 Morse SS. 1993. Examining the origins of emerging viruses. Pages 10–28 in Morse SS, editor.
540 Emerging Viruses. Oxford University Press, New York.
541 Morse SS. 1995. Factors in the emergence of infectious diseases. Emerging Infectious Diseases
542 **1:**7–15.

543 Morse SS. 2004. Factors and determinants of disease emergence. Scientific and Technical
544 Review of the Office International des Epizooties **23:**443–451.
545 Muller LK, Lorch JM, Linder DL, O'Connor M, Gargas A, Blehert DS. 2012. Bat white-nose
546 syndrome: a real-time TaqMan polymerase chain reaction test targeting the intergenic
547 spacer region of *Geomyces destructans*. Mycologia **105:**253–259.
548 Parratt SR, Numminen E, Laine A-L. 2016. Infectious disease dynamics in heterogeneous
549 landscapes. Annual Review of Ecology, Evolution, and Systematics **47:**283–306.
550 Perez L, Dragicevic S. 2009. An agent-based approach for modeling dynamics of contagious
551 disease spread. International Journal of Health Geographics **8:**50.
552 Perry RW. 2013. A review of factors affecting cave climates for hibernating bats in temperate
553 North America. Environmental Reviews **21:**28–39.
554 Pettit JL, O'Keefe JM. 2017. Impacts of white-nose syndrome observed during long-term
555 monitoring of a midwestern bat community. Journal of Fish and Wildlife Management
556 **8:**69–78.
557 Raudabaugh DB, Miller AN. 2013. Nutritional capability of and substrate suitability for
558 *Pseudogymnoascus destructans*, the causal agent of bat white-nose syndrome. PLOS One
559 **8:**e78300.
560 Reynolds HT, Ingersoll T, Barton HA. 2015. Modeling the environmental growth of
561 *Pseudogymnoascus destructans* and its impact on the white-nose syndrome epidemic.
562 Journal of Wildlife Diseases **51:**318–331.
563 Sandel JK, Benatar GR, Burke KM, Walker CW, Lacher Jr TE, Honeycutt RL. 2001. Use and
564 selection of winter hibernacula by the eastern pipistrelle (*Pipistrellus subflavus*) in Texas.
565 Journal of Mammalogy **82:**173–178.

566 Schmidly DJ, Bradley RD. 2016. The mammals of Texas. University of Texas. University of
567 Texas Press, Austin, Texas.
568 Smith DL, Lucey B, Waller LA, Childs JE, Real LA. 2002. Predicting the spatial dynamics of
569 rabies epidemics on heterogeneous landscapes. Proceedings of the National Academy of
570 Sciences **99:**3668–3672.
571 Sunnåker M, Busetto AG, Numminen E, Corander J, Foll M, Dessimoz C. 2013. Approximate
572 Bayesian Computation. PLOS Computational Biology **9:**e1002803.
573 TPWD (Texas Parks and Wildlife Department). 2017. Fungus that causes white-nose syndrome
574 in bats detected in Texas. Austin, Texas. Available from
575 https://tpwd.texas.gov/newsmedia/releases/?req=20170323c (accessed March 2020).
576 TPWD (Texas Parks and Wildlife Department). 2018. Fungus causing white-nose syndrome
577 spreads into central Texas. Austin, Texas. Available from
578 https://tpwd.texas.gov/newsmedia/releases/?req=20180404a (accessed November 2020).
579 TPWD (Texas Parks and Wildlife Department). 2019. Fungus causing white-nose syndrome in
580 bats continues to spread in Texas. Austin, Texas. Available from
581 https://tpwd.texas.gov/newsmedia/releases/?req=20190508a (accessed March 2020).
582 TPWD (Texas Parks and Wildlife Department). 2020. White-nose syndrome confirmed in bats in
583 Texas. Austin, Texas. Available from
584 https://tpwd.texas.gov/newsmedia/releases/?req=20200305a (accessed June 2020).
585 Thogmartin WE, Sanders-Reed CA, Szymanski JA, McKann PC, Pruitt L, King RA, Runge MC,
586 Russell RE. 2013. White-nose syndrome is likely to extirpate the endangered Indiana bat
587 over large parts of its range. Biological Conservation **160:**162–172.

588 Tompkins DM, Carver S, Jones ME, Krkošek M, Skerratt LF. 2015. Emerging infectious
589 diseases of wildlife: a critical perspective. Trends in Parasitology **31:**149–159.
590 Tinkle DW, Milstead WW. 1960. Sex ratios and population density in hibernating myotis. The
591 American Midland Naturalist **63:**327–334.
592 Turner GG, Reeder DM. 2009. Update of white-nose syndrome in bats. Bat Research News
593 **50:**47–53.
594 Verant ML, Boyles JG, Waldrep, Jr W, Wibbelt G, Blehert DS. 2012. Temperature-dependent
595 growth of *Geomyces destructans*, the fungus that causes bat white-nose syndrome. PLOS
596 One **7:**e46280.
597 Verant ML, Meteyer CU, Speakman JR, Cryan PM, Lorch JM, Blehert DS. 2014. White-nose
598 syndrome initiates a cascade of physiological disturbances in the hibernating bat host.
599 BMC Physiology **14:**10.
600 Walker CW, Sandel JK, Honeycutt RL, Adams C. 1996. Winter utilization of box culverts by
601 vespertilionid bats in southeast Texas. Texas Academy of Science **48**:166–168.
602 Warnecke L, Turnera JM, Bollingerb TK, Lorch JM, Misra V, Cryan PM, Wibbelt G, Blehert
603 DS, Willis CKR. 2012. Inoculation of bats with European *Geomyces destructans* supports
604 the novel pathogen hypothesis for the origin of white-nose syndrome. PNAS **109:**6999–
605 7003.
606 Wilder AP, Frick WF, Langwig KE, Kunz TH. 2011. Risk factors associated with mortality from
607 white-nose syndrome among hibernating bat colonies. Biology Letters **7:**950–953.

608 Table 1. The model parameters and our value estimates after validation step based on 2020 WNS survey data (see Materials and
609 Methods for details). Parameter values are the averaged estimates based on referenced publications and approximated values, and are
610 scaled by the carrying capacity (thus do not directly match values in references).

Symbol	Parameter name	Unit	Value(s)	Reference
$\hat{r}_h$	Bat population growth rate	day^{-1}	0.00333	Fenton and Barclay 1980; Reynolds et al. 2015
r_f	Fungal growth rate	day^{-1}	0.00152	Approximated
β_e	Environmental transmission rate	(unit fungi)$^{-1}$ day^{-1}	0.043	Reynolds et al. 2015
β_d	Direct transmission rate	(unit bats)$^{-1}$ day^{-1}	0.195	Lorch et al. 2011 Langwig et al. 2012, 2015; Frick et al. 2015
μ_h	Hibernation mortality	day^{-1}	0.0012	Webb et al. 1996
μ_f	Disease mortality	day^{-1}	0.039	Approximated
λ	Fungal shedding	(unit bats)$^{-1}$ day^{-1}	0.017	Approximated
δ_e	Recovery (exposed to susceptible)	day^{-1}	0.0488	Fuller et al. 2012; Carpenter et al. 2016
δ_n	Recovery (infectious to exposed)	day^{-1}	0.0225	Fuller et al. 2012; Carpenter et al. 2016; Ballmann et al. 2017
φ	Infection rate	day^{-1}	0.0755	Fuller et al. 2012; Carpenter et al. 2016
ρ	Migration proportion	-	0.042	Approximated
γ	Migration distribution parameter	-	0.00868	Approximated
init s	Prop. susceptible bats in initially affected counties	-	0.7	Approximated based on swab survey results
init e	Prop. exposed bats in initially affected counties	-	0.28	Approximated based on swab survey results
init n	Prop. infectious bats in initially infected counties	-	0.02	Approximated based on swab survey results
init f	Free-living fungus in initially affected counties	-	0.1	Approximated
$\eta^o_{h\leftarrow a,1}$	Ambient temp. threshold 1	^{o}C	11.5	Perry 2013; Meierhofer et al. 2019
$\eta^o_{h\leftarrow a,2}$	Ambient temp. threshold 2	^{o}C	12.5	Perry 2013; Meierhofer et al. 2019

$\eta^{c}_{h\leftarrow a}$	Hibernaculum temp. threshold	^{o}C	11.5	Perry 2013; Meierhofer et al. 2019
$\widehat{\omega}_{a\leftarrow h}$	Activation rate	day^{-1}	0.1	Approximated
$\widehat{\omega}_{h\leftarrow a}$	Hibernation rate	day^{-1}	0.1	Approximated

611

Figure 1. A conceptual drawing of the model spatial setting. The top part shows binning of hibernacula by the within cave mean temperatures according to a Gaussian distribution obtained from a linear model for each county j. Each bin becomes a patch i with a given mean within cave temperature T^{c}_{i,j} and capacity K_{i,j}. In the bottom part, dispersal distances between counties j are the distances between the county midpoints (grey and colored circles).

Figure 2. Texas counties where white-nose syndrome (WNS) was detected in 2020 (dark red), where only *P. destructans* was detected in 2020 (medium red), where *P. destructans* was detected in previous years (light red), and counties surveyed in Texas where neither WNS nor *P. destructans* was detected (gray).

Figure 3. Interpolation of the carrying-capacity-scaled infection output for (**a**) 5 and (**b**) 10 years of simulation. Grey tiles show regions of 0 predicted infection. Interpolation predicts for values within a convex hull around the county centerpoints (black dots). Sites with observed infection data in 2008 marked with a circle around the point. Interpolation of the proportional loss of bats relative to infection-free model for (**c**) 5 and (**d**) 10 years. Gradient scale of heat map weighted to distinguish between larger degrees of loss (50%+).

Figure 4. Effects of the disease on counties at different latitudes. Proportion of surviving bats (a) and the amount of free-living fungus (b), averaged for each county. The effects after 5 and 10 years are marked with blue and red dots, respectively. The matching counties are connected by dotted lines. Counties initiated with the disease are marked with a black circle around the dot. The y-axis scale on panel B is in units of fungal carrying capacity.

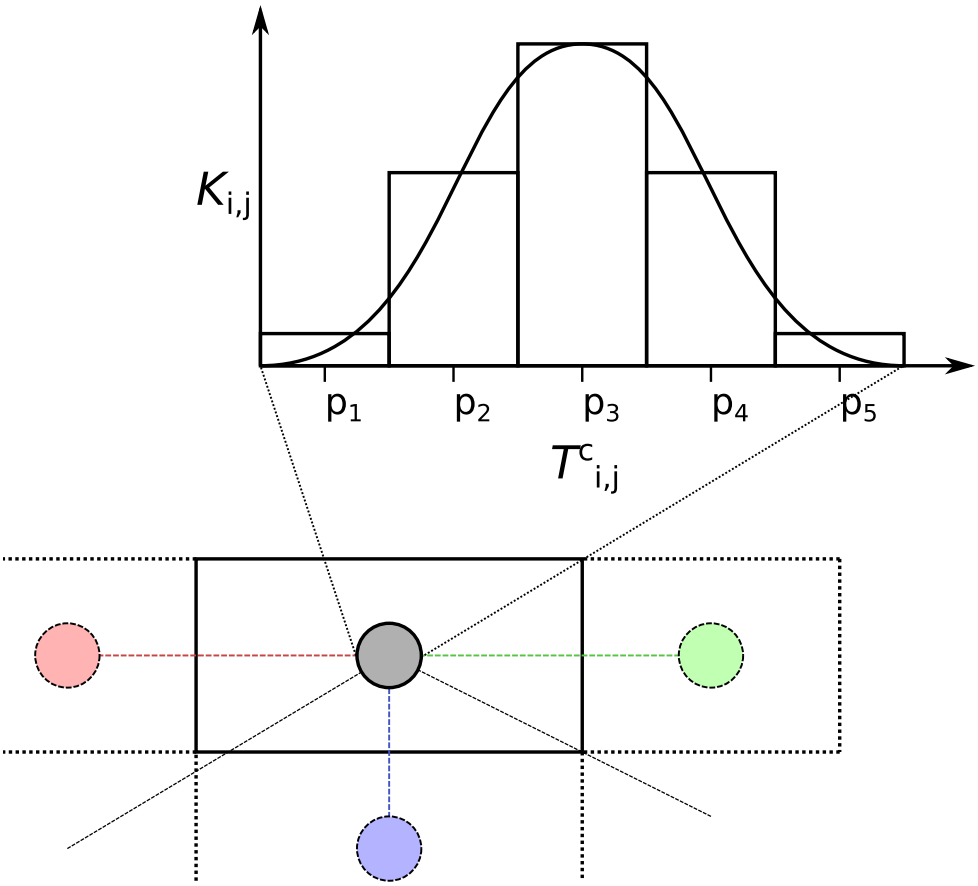

Figure 1. A conceptual drawing of the model spatial setting. The top part shows binning of hibernacula by the within cave mean temperatures according to a Gaussian distribution obtained from a linear model for each county j. Each bin becomes a patch i with a given mean within cave temperature T^{c}_{i,j} and capacity K_{i,j}. In the bottom part, dispersal distances between counties j are the distances between the county midpoints (grey and colored circles).

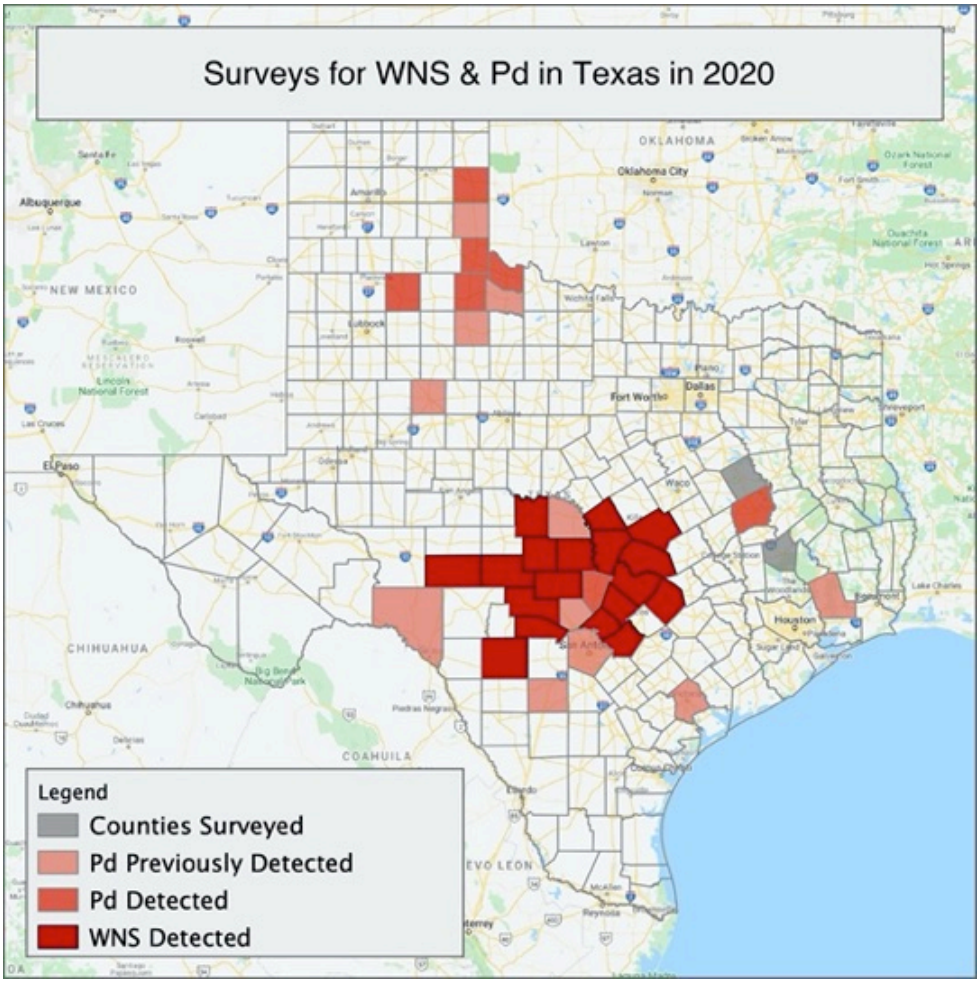

Figure 2. Texas counties where white-nose syndrome (WNS) was detected in 2020 (dark red), where only *P. destructans* was detected in 2020 (medium red), where *P. destructans* was detected in previous years (light red), and counties surveyed in Texas where neither WNS nor *P. destructans* was detected (gray).

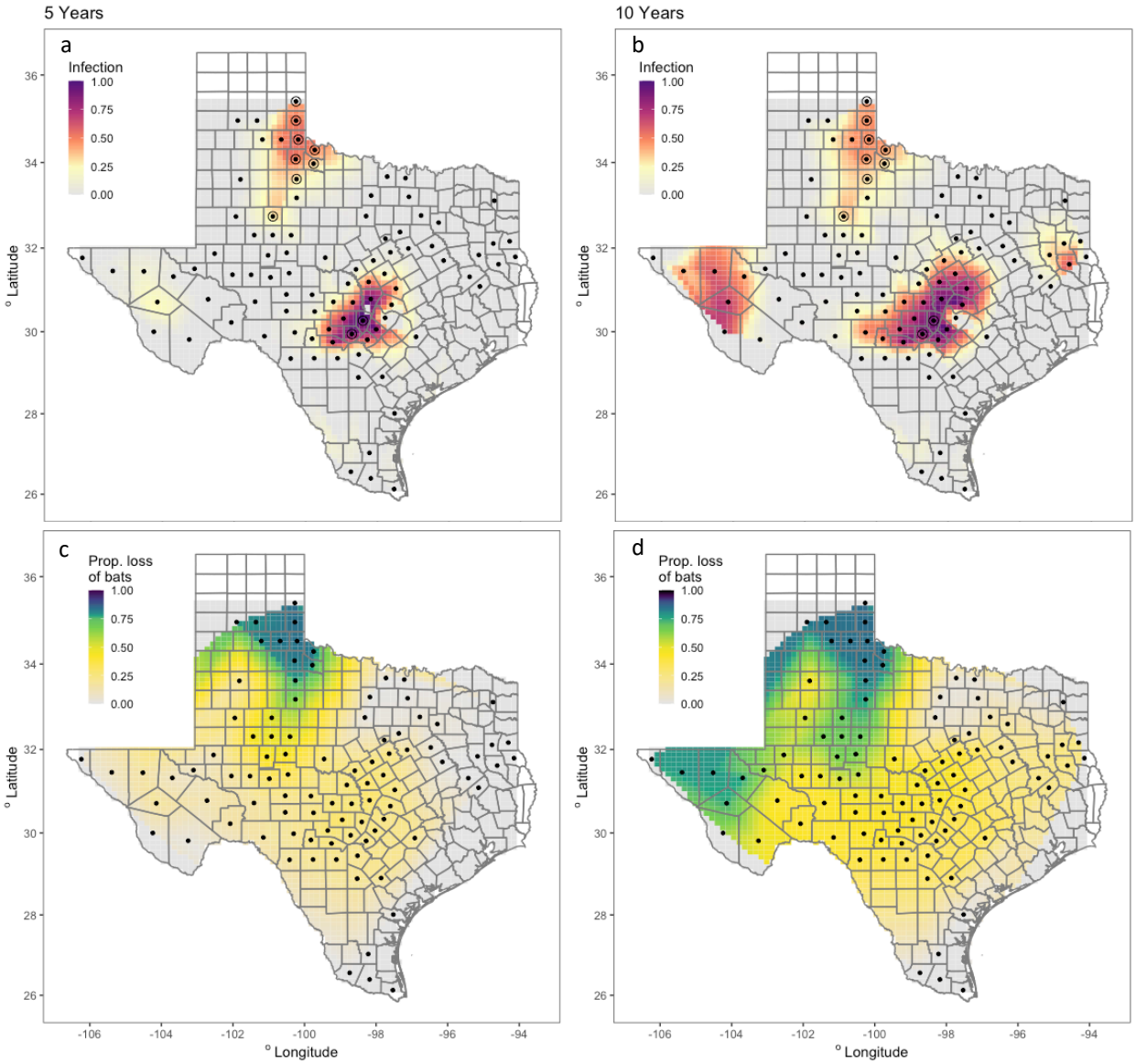

Figure 3. Interpolation of the carrying-capacity-scaled infection output for (**a**) 5 and (**b**) 10 years of simulation. Grey tiles show regions of 0 predicted infection. Interpolation predicts for values within a convex hull around the county centerpoints (black dots). Sites with observed infection data in 2008 marked with a circle around the point. Interpolation of the proportional loss of bats relative to infection-free model for (**c**) 5 and (**d**) 10 years. Gradient scale of heat map weighted to distinguish between larger degrees of loss (50% +).

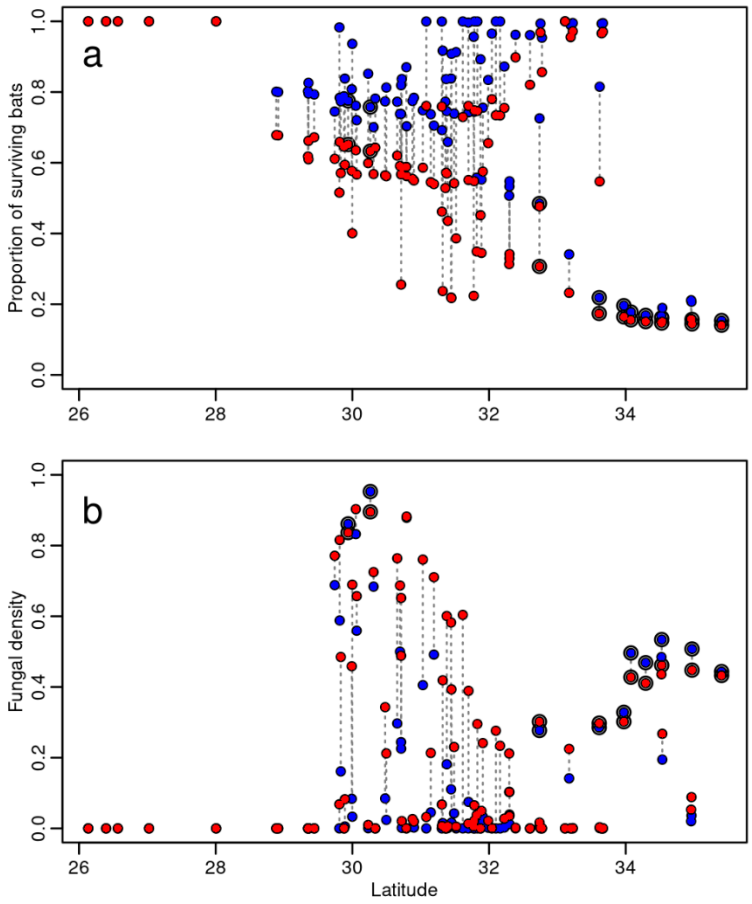

Figure 4. Effects of the disease on counties at different latitudes. Proportion of surviving bats (panel a) and the amount of free-living fungus (panel b), averaged for each county. The effects after 5 and 10 years are marked with blue and red dots, respectively. The matching counties are connected by dotted lines. Counties initiated with the disease are marked with a black circle around the dot. The y-axis scale on panel B is in units of fungal carrying capacity.